ISSN 1996-3343

Asian Journal of Applied Sciences

http://knowledgiascientific.com

Knowledgia SCIENTIFIC
A Place to Publish Outstanding Research

Asian Journal of Applied Sciences 1 (2): 93-109, 2008
ISSN 1996-3343

Bi-Hierarchical Finite Element for the Analysis of the non Axisymetric Free Vibration of Shells of Revolution

[1]Mohammed Nabil Ouissi and [2]Abderrahim Houmat
[1]Laboratoire Eau et Ouvrages Dans Leurs Environnements,
University of Abou Bekr, Belkaïd, Tlemcen, Algéria
[2]Laboratoire d'automatique, University of Abou Bekr, Belkaïd, Tlemcen, Algéria

Abstract: A new hierarchical finite element is developed to analyze the free vibration of isotropic shells of revolution with linear varying thickness. It is a bi-hierarchical four nodes quadrilateral element with three degrees of freedom (three displacements) by node. The specificity of this element is a double increase of the hierarchical mode number independently according to both axial and radial directions. The advantage is that the solution is accurate for high ratio dimensions as well flattened axisymmetric (plates) shells that slim ones (high cylindrical shells) with different shapes and boundary conditions. The second advantage is the possibility of using only one element to idealize regular shape shells. Through the application of this element to some numerical examples, the comparisons with other studies show clearly that this element gives good results accuracy with simple idealization for axisymmetric and non-axisymmetric shells vibration (thick and thin).

Key words: Hierarchical finite element method, double hierarchical increment, shells of revolution, non-axisymmetric, free vibration

INTRODUCTION

The propose of this study is to present a new bi-hierarchical finite element to idealize isotropic shells of revolution with linear varying thickness. Shells of revolution can be of different shape and dimensions. Thin and thick plates and cylindrical shells can not be idealized by the same finite elements in standard or hierarchical method. The dimensions ratio and the shape of the shell influence on the choice of the finite element and the mesh. For modeling for example a storage tank, one must have two elements, one for the cylinder and the other for the plate. The new proposed element can idealize the two shells.

The literature on finite element approximation of shells of revolution is huge. Let us just mention a few different approaches.

Bodies of revolution compounds of thin shell segments, thick shell segments and rings have been analyzed by using Mindlin Reissner axisymetric finite elements which take in account the shearing strains and the rotationnal inertia effects (Özakça and Hinton, 1993).

To predict the natural frequencies of shells of revolution which may have arbitrary shape of meridian, general type of material property and any kind of boundary condition, a substructuring analysis method was presented (Tan, 1998). The method was developed in the context of first order shear deformation shell theory as well as the classical thin shell theory.

Other methods were implemented of which a three-dimensional method of analysis to determine the frequencies and eigen modes of hollow bodies of revolution with arbitrary shell curvatures and

Corresponding Author: Mohammed Nabil Ouissi, Engineering Sciences Faculty, University of Abou Bekr, Belkaïd-Tlemcen Algéria, BP 230 Chetouane, Tlemcen 13000, Algeria
Tel: 0213790035094 Fax: 021343285685

arbitrarily varying curvatures (Leissa, 1999). A three-dimensional shell theory applicable to doubly curved thick open shell which are arbitrarily deep in one principal direction but are shallow in the other direction, used Ritz variational formulation with algebraic polynomials as trial functions to have the natural frequencies (Young, 2000). Solid and hollow hemi-ellipsoids of revolution (the hollow ones being shells) with and without an axially circular cylindrical hole (Shim and Kang, 2004), paraboloïd solids and paraboloïd shells of revolution with variable thickness (Kang and Leissa, 2005a), thick and complete (not truncated) conical shells of revolution (Kang and Leissa, 2005b) and hyperboloidal shells of revolution (Kang and Leissa, 2005c) were analysed by methods based upon the 3-D dynamic equations of elasticity. The Ritz method was used to solve the eigenvalue problem.

A variety of finite elements was presented for shells of revolution such as the facet elements, the linear truncated elements based on the theory of Kirchhoff and the truncated elements with double curve based on the theory of Mindlin-Reissner (Batoz and Dhatt, 1992). The truncated elements are either with two displacements and a rotation by node, or with three displacements and a rotation, or finally for the not-axisymmetric case with three displacements and a rotation.

This study gives the possibility of idealize most of shells of revolution by only one element. The proposed element in this study is a four nodes volumetric and axisymmetric bi-hierarchical finite element with only displacements as degrees of freedom. The word bi-hierarchical comes from the fact that this element has two hierarchical mode numbers, one in the axis direction and the second in the radius direction.

These two hierarchical mode numbers increase independently. This element can than idealize flattened shells like plates and high shells like cylinders and conical shells (thins and thicks) or structures composed of them. For the first kind of shells, the radius direction hierarchical mode number is increased to have the accuracy of the results and for the second kind, the axis hierarchical mode number is increased.

This element gives the possibility of reducing the mesh. The accuracy is not given by a high number of elements but only by increasing the two hierarchical mode numbers. Shells of revolution are of different kinds, shapes, thickness and boundary conditions. An axisymmetric structure composed of shells of revolution with constant or linearly varying thickness can be also idealized by an only one finite element. The shape displacement is defined by a double hierarchical increment.

FORMULATIONS

Potential Energy

The potential energy stored in the shell is in the form of a strain energy due to the effect of both stretching and bending. The strain energy expression can be written as:

$$U(t)=\frac{1}{2}\int_{R_i}^{R_e}\int_{0}^{H}\int_{0}^{2\pi}\left(\sigma_r\varepsilon_r+\sigma_z\varepsilon_z+\sigma_\theta\varepsilon_\theta+\tau_{rz}\gamma_{rz}+\tau_{r\theta}\gamma_{r\theta}+\tau_{z\theta}\gamma_{z\theta}\right).r.dr.dz.d\theta \tag{1}$$

And in matrix form

$$U(t)=\frac{1}{2}\int_{R_i}^{R_e}\int_{0}^{H}\int_{0}^{2\pi}\left(\{\varepsilon\}^T.\{\sigma\}\right).r.dr.dz.d\theta \tag{2}$$

Where:

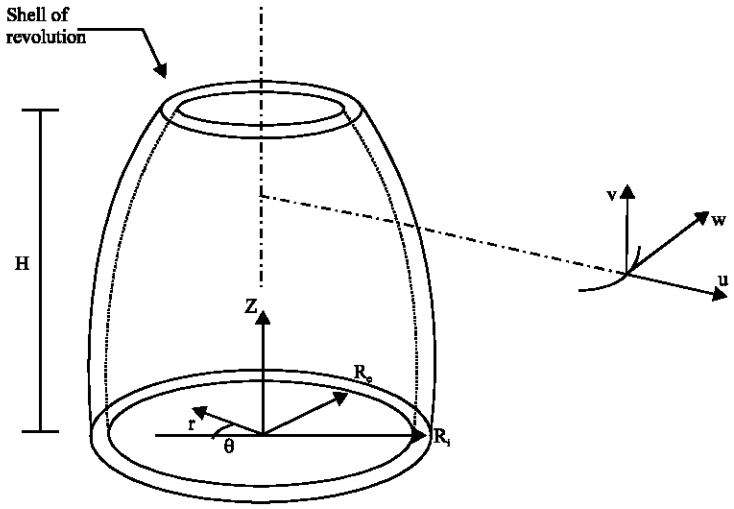

Fig. 1: Shell of revolution

$$\{\varepsilon\} = \begin{Bmatrix} \varepsilon_r \\ \varepsilon_z \\ \varepsilon_\theta \\ \gamma_{rz} \\ \gamma_{r\theta} \\ \gamma_{z\theta} \end{Bmatrix} \quad \text{and} \quad \{\sigma\} = \begin{Bmatrix} \sigma_r \\ \sigma_z \\ \sigma_\theta \\ \tau_{rz} \\ \tau_{r\theta} \\ \tau_{z\theta} \end{Bmatrix} \tag{3}$$

are the stain and stress vectors

The constitutive relationship between stress and strain is the generalized Hooke's law. For an isotropic homogeneous structure, it is given as:

$$\{\sigma\} = [D].\{\varepsilon\} \tag{4}$$

where, [D] is the elasticity matrix given by:

$$[D] = \frac{E}{(1+\nu).(1-2\nu)} \begin{bmatrix} 1-\nu & \nu & \nu & 0 & 0 & 0 \\ \nu & 1-\nu & \nu & 0 & 0 & 0 \\ \nu & \nu & 1-\nu & 0 & 0 & 0 \\ 0 & 0 & 0 & \frac{1-2\nu}{2} & 0 & 0 \\ 0 & 0 & 0 & 0 & \frac{1-2\nu}{2} & 0 \\ 0 & 0 & 0 & 0 & 0 & \frac{1-2\nu}{2} \end{bmatrix} \tag{5}$$

E is Young's modulus and υ is Poisson ratio of the structure.

Equation 4 into Eq. 2, the potential energy is given in terms of strain as:

$$U(t) = \frac{1}{2} \int_{R_i}^{R_o} \int_{0}^{H} \int_{0}^{2\pi} \left(\{\varepsilon\}^T .[D].\{\varepsilon\} \right) .r.dr.dz.d\theta \tag{6}$$

The strain-displacement relations are given by:

$$\{\varepsilon\} = \begin{Bmatrix} \varepsilon_r \\ \varepsilon_z \\ \varepsilon_\theta \\ \gamma_{rz} \\ \gamma_{r\theta} \\ \gamma_{z\theta} \end{Bmatrix} = \begin{Bmatrix} \dfrac{\partial u}{\partial r} \\ \dfrac{\partial v}{\partial z} \\ \dfrac{u}{r} + \dfrac{1}{r}.\dfrac{\partial w}{\partial \theta} \\ \dfrac{\partial u}{\partial z} + \dfrac{\partial v}{\partial r} \\ \dfrac{1}{r}.\dfrac{\partial u}{\partial \theta} + \dfrac{\partial w}{\partial r} - \dfrac{w}{r} \\ \dfrac{1}{r}.\dfrac{\partial v}{\partial \theta} + \dfrac{\partial w}{\partial z} \end{Bmatrix} \tag{7}$$

The strain vector can be expressed in terms of the displacement vector as follows:

$$\{\varepsilon\} = [d].\{\delta\} \tag{8}$$

Where:

$$\{\delta\} = \{u, v, w\} \tag{9}$$

and [d] is a differential operator matrix defined by:

$$\{d\} = \begin{bmatrix} \dfrac{\partial}{\partial r} & 0 & 0 \\ 0 & \dfrac{\partial}{\partial z} & 0 \\ \dfrac{1}{r} & 0 & \dfrac{1}{r}.\dfrac{\partial}{\partial \theta} \\ \dfrac{\partial}{\partial z} & \dfrac{\partial}{\partial r} & 0 \\ \dfrac{1}{r}.\dfrac{\partial}{\partial \theta} & 0 & \dfrac{\partial}{\partial r} - \dfrac{1}{r} \\ 0 & \dfrac{1}{r}.\dfrac{\partial}{\partial \theta} & \dfrac{\partial}{\partial z} \end{bmatrix} \tag{10}$$

The stress vector can be expressed in terms of the displacement vector, as:

$$\{\sigma\} = \frac{E}{(1+\nu).(1-2\nu)}.\begin{Bmatrix} (1-\nu).\dfrac{\partial u}{\partial r} + \nu.\left(\dfrac{\partial v}{\partial z} + \dfrac{u}{r} + \dfrac{1}{r}.\dfrac{\partial w}{\partial \theta}\right) \\ (1-\nu).\dfrac{\partial v}{\partial z} + \nu.\left(\dfrac{\partial u}{\partial r} + \dfrac{u}{r} + \dfrac{1}{r}.\dfrac{\partial w}{\partial \theta}\right) \\ (1-\nu).\left(\dfrac{u}{r} + \dfrac{1}{r}.\dfrac{\partial w}{\partial \theta}\right) + \nu.\left(\dfrac{\partial u}{\partial r} + \dfrac{\partial v}{\partial z}\right) \\ \dfrac{1-2\nu}{2}.\left(\dfrac{\partial u}{\partial z} + \dfrac{\partial v}{\partial r}\right) \\ \dfrac{1-2\nu}{2}.\left(\dfrac{1}{r}.\dfrac{\partial u}{\partial \theta} + \dfrac{\partial w}{\partial r} - \dfrac{w}{r}\right) \\ \dfrac{1-2\nu}{2}.\left(\dfrac{1}{r}.\dfrac{\partial v}{\partial \theta} + \dfrac{\partial w}{\partial z}\right) \end{Bmatrix} \tag{11}$$

Kinetic Energy

The kinetic energy of the shell can be written as:

$$T(t)=\frac{1}{2}\int_{R_i}^{R_e}\int_{0}^{H}\int_{O}^{2\pi}\rho.\left[\left(\frac{\partial u(r,z,\theta,t)}{\partial t}\right)^2+\left(\frac{\partial v(r,z,\theta,t)}{\partial t}\right)^2+\left(\frac{\partial w(r,z,\theta,t)}{\partial t}\right)^2\right].r.dr.dz.d\theta \tag{12}$$

where ρ is the density. Equation can be written as follows:

$$T(t)=\frac{1}{2}\int_{R_i}^{R_e}\int_{0}^{H}\int_{O}^{2\pi}\rho.\{\dot{\delta}\}^T.\{\dot{\delta}\}.r.dr.dz.d\theta \tag{13}$$

where, $\{\delta\}$ is the displacement vector defined by Eq. 9 and differentiation is with respect to the time, t.

Hierarchical Finite Element Formulation

The hierarchical finite element method known under the name of the p-version of the finite element method is more precise and its convergence is faster than that of the h-method. Indeed, when the exact solution is analytical everywhere the rate of convergence is exponential, whereas that of the h-method is only algebraic. The quality of the solutions is not very sensitive to the distortions of the elements, which allows the use of flattened elements or great ratio on sides without penalizing the precision too much. In addition, as a hierarchical formulation is adopted for the representation of displacements, the matrix of stiffness relative to a given degree imbricates those of lower degrees. This makes it possible to obtain in an economic way a sequence of solutions instead of only one solution as it is the case of the h-method (Babuska and Szabo, 1982; Szabo, 1990; Szabo and Babuska, 1991).

The hp version of the finite element method has as a characteristic to increase the precision by increasing both the degree of the polynomial of interpolation and the number of finite elements as for the standard finite element method (Szabo and Babuska, 1991).

Idealization of the Shell

The shell is divided into four nodes hierarchical axisymmetric quadrilateral isoparametric finite elements (Fig. 3). The element size is arbitrary. They may all be of the same size or may all be different. The shell can also be idealized by only one element if the thickness of the shell is varying linearly or if it is constant.

The equation of motion of the shell admit the representation of the Radial, circumferential and axial displacement components u, v and w (Fig. 2) following respectively R, Z and è in the following form:

$$\begin{cases} u(r,z,\theta)=\bar{u}(r,z).\cos n\theta \\ v(r,z,\theta)=\bar{v}(r,z).\cos n\theta \\ w(r,z,\theta)=\bar{w}(r,z).\sin n\theta \end{cases} \tag{14}$$

The time dependence is removed by assuming that the displacements vary sinusoidally in phase at the same frequency. The displacement functions $\bar{u}(r,z),\bar{v}(r,z)$ and $\bar{w}(r,z)$ can be expressed in terms of the nodal displacements of the finite elements by means of an appropriate set of interpolation functions.

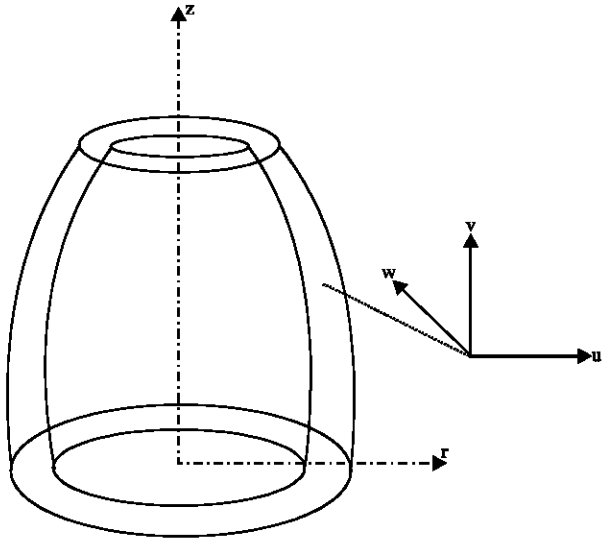

Fig. 2: Displacements of a shell point

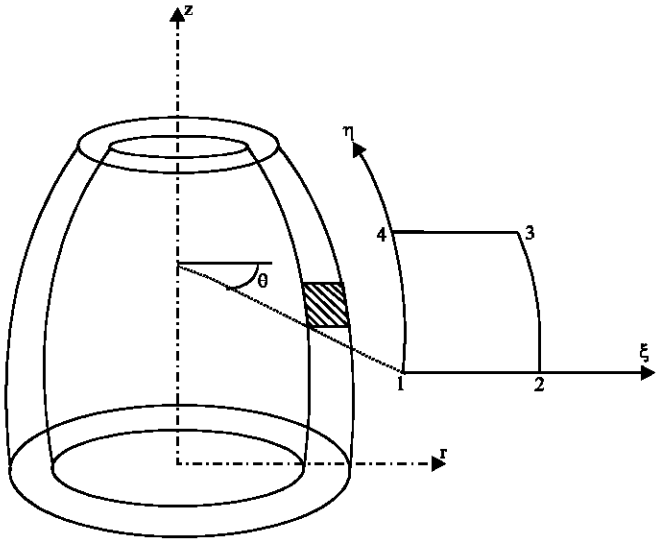

Fig. 3: Cylindrical and non-dimensional coordinates

Shape Functions Selection

The hierarchical shape functions are generally selected in the Serendipity space. In this paper, the shape functions are built from the shifted Legendre orthogonal polynomials introduced by (Houmat, 2004). These polynomials are defined in the interval [0,1].

They can be classified in three categories:

- Nodal shape functions
- Side shape functions
- Internal shape functions

Their recurring form is:

$$\begin{cases} f_1(x) = 1 - x \\ f_1(x) = x \\ f_{i+2}(x) = \int_0^x P_i(\alpha).d\alpha \end{cases} \tag{15}$$

where $P_i(\alpha)$ are the shifted Legendre polynomials defined by:

$$\begin{cases} P_0(\alpha) = 1 \\ P_1(\alpha) = 2.\alpha - 1 \\ P_{i+1}(\alpha) = \frac{1}{i+1} \cdot \left[(-2i - 1 + (4i+2)\alpha) \cdot P_i(\alpha) - i \cdot P_{i-1}(\alpha) \right] \quad i = 1,2,3,.. \end{cases} \tag{16}$$

The shape functions are given on the basis of one-dimensional hierarchical finite element. The origin of the non-dimensional coordinates is at the left end of the element. For the C° continuous problems, the first two linear shape functions of the standard finite element method are retained. The higher order C° shape functions vanish at each end of the elements, they are used to describe the displacement function inside the element. These functions are generated by using the recursive formula (16).

The first six hierarchical shape functions are represented in the Table 1.

Having the shape functions, the displacement functions $\bar{u}(r,z)$, $\bar{v}(r,z)$ and $\bar{w}(r,z)$ can be expressed:

$$\begin{cases} \bar{u}(r,z) = \sum_1^n N_i(r,z).u_i \\ \bar{v}(r,z) = \sum_1^n N_i(r,z).v_i \\ \bar{w}(r,z) = \sum_1^n N_i(r,z).w_i \end{cases} \tag{17}$$

Where:

$$N_i(r,z) = f_k(r).g_l(z) \tag{18}$$

with:

k = 1,..,p+1 and l = 1,..,q+1
p = Hierarchical modes number according to ξ
q = Hierarchical modes number according to η
f, g = Shape functions

The matrix form of the expression (17) is:

$$\{\bar{\delta}\} = [N].\{q\} \tag{19}$$

Where:

$$\{\bar{\delta}\} = \begin{Bmatrix} \bar{u}(r,z) \\ \bar{v}(r,z) \\ \bar{w}(r,z) \end{Bmatrix} \tag{20}$$

Table 1: The first six hierarchical shape functions

No. of Hierarchical modes	Shape functions in terms of Shifted-Legendre polynomials	Graphic representation
1	$1-\xi$	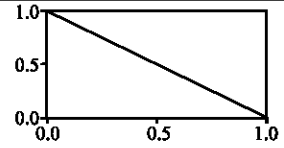
2	ξ	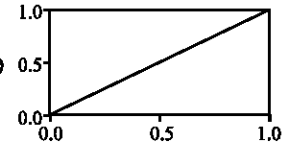
3	$\xi^2-\xi$	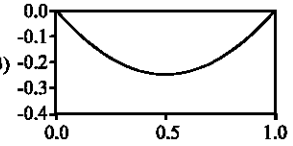
4	$2\xi^3-3\xi^2+\xi$	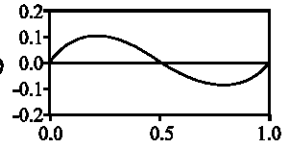
5	$5\xi^4-10\xi^3+6\xi^2-\xi$	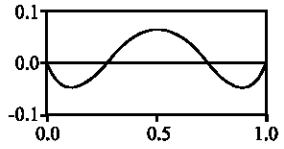
6	$14\xi^5-35\xi^4+30\xi^3-10\xi^2+\xi$	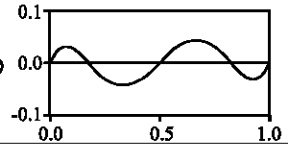

is the generalized displacement vector,

$$\{q\} = \{u_1, v_1, w_1, ..., u_i, v_i, w_i, ...\}^T \tag{21}$$

With i = 1,…,(p+1)(q+1)
is the nodal displacement vector
And

$$[N] = \left[[N_1], [N_2], ..., [N_i], ..., \left[N_{(p+1)(q+1)}\right]\right] \tag{22}$$

is the shape functions matrix, where $[N_i]$ is a sub-matrix given by:

$$[N_i]=\begin{bmatrix} f_k(r).g_l(z) & 0 & 0 \\ 0 & f_k(r).g_l(z) & 0 \\ 0 & 0 & f_k(r).g_l(z) \end{bmatrix} \tag{23}$$

$f_k(r)$ and $g_l(z)$ are the nodal, side and internal shape functions of the element.

Shell Stiffness Matrix

Defining the stiffness properties of the shell is reduced to evaluating the stiffness of a typical element.

Expression (14) can be written

$$\{\delta\}=[\theta_n].\{\bar{\delta}\} \tag{24}$$

Where:

$$[\theta_n]=\begin{bmatrix} \cos n\theta & 0 & 0 \\ 0 & \cos n\theta & 0 \\ 0 & 0 & \sin n\theta \end{bmatrix} \tag{25}$$

Substitute Eq. 24 into Eq. 8, then one can write

$$\{\varepsilon\}=[d].\{\delta\}=[d].[\theta_n].\{\bar{\delta}\}=[\bar{d}].\{\bar{\delta}\} \tag{26}$$

Where:

$$[\bar{d}]=\begin{bmatrix} \frac{\partial}{\partial r}\cos n\theta & 0 & 0 \\ 0 & \frac{\partial}{\partial z}\cos n\theta & 0 \\ \frac{1}{r}\cos n\theta & 0 & \frac{n}{r}\cos n\theta \\ \frac{\partial}{\partial z}\cos n\theta & \frac{\partial}{\partial r}\cos n\theta & 0 \\ -\frac{n}{r}\sin n\theta & 0 & \left(\frac{\partial}{\partial r}-\frac{1}{r}\right)\sin n\theta \\ 0 & -\frac{n}{r}\sin n\theta & \frac{\partial}{\partial z}\sin n\theta \end{bmatrix} \tag{27}$$

Equation 26 into Eq. 6, the potential energy can be written, as

$$U(t)=\frac{1}{2}\int_{R_1}^{R_2}\int_0^H\int_0^{2\pi}\left(\left([\bar{d}].\{\bar{\delta}\}\right)^T.[D].[\bar{d}].\{\bar{\delta}\}\right).r.dr.dz.d\theta \tag{28}$$

To evaluate the stiffness matrix of an element, the global cylindrical coordinates (r , z) may be expressed in terms of the local dimensionless coordinates (ξ, η) by:

$$\begin{cases} r=(1-\xi).(1-\eta).r_1+\xi.(1-\eta)r_2+\xi.\eta.r_3+(1-\xi).\eta.r_4 \\ z=(1-\xi).(1-\eta).z_1+\xi.(1-\eta)z_2+\xi.\eta.z_3+(1-\xi).\eta.z_4 \end{cases} \tag{29}$$

Where r_i and z_i are the cylindrical coordinates of the element nodes

The coordinates ξ and η used to define the element geometry are given by the Fig. 3. They are varying from 0 to 1 whose origin is the node lower right of the element.

The derivatives can be written using the Jacobian matrix:

$$\begin{Bmatrix} \frac{\partial}{\partial \xi} \\ \frac{\partial}{\partial \eta} \end{Bmatrix} = [J].\begin{Bmatrix} \frac{\partial}{\partial r} \\ \frac{\partial}{\partial z} \end{Bmatrix} \tag{30a}$$

Where:

$$[J] = \begin{bmatrix} \frac{\partial r}{\partial \xi} & \frac{\partial z}{\partial \xi} \\ \frac{\partial r}{\partial \eta} & \frac{\partial z}{\partial \eta} \end{bmatrix} \tag{30b}$$

And then after mathematical transformations, one can write

$$r.dr.dz.d\theta = k.\pi.|J|.r.d\xi.d\eta \tag{31}$$

where, k = 2 for n = 0 and k = 1 for n = 1,2,… (n: circumferential wave number)
Equation 31 and 19 into Eq. 28, the potential energy can be written, as:

$$U(t) = \frac{k\pi}{2}\int_0^1\int_0^1 \left(\{q\}^T.[N]^T.\left[\bar{d}\right]^T.[D].\left[\bar{d}\right].[N].\{q\}\right).|J|.r.d\xi.d\eta \tag{32a}$$

$$= \frac{1}{2}\{q\}^T.\left[k\pi.\int_0^1\int_0^1 \left(.[N]^T.\left[\bar{d}\right]^T.[D].\left[\bar{d}\right].[N].\right).|J|.r.d\xi.d\eta\right].\{q\} \tag{32b}$$

$$= \frac{1}{2}\{q\}^T.[K].\{q\} \tag{32c}$$

Where:

$$[K_e] = k\pi.\int_0^1\int_0^1 \left([B]^T.[D].[B]\right).|J|.r.d\xi.d\eta.d\theta \tag{33}$$

is the element stiffness matrix
and

$$[B] = \left[\bar{d}\right].[N] \tag{34a}$$

$$= \left[\bar{d}\right].\left[[N_1],[N_2],...,[N_i],...,\left[N_{(p+1)(q+1)}\right]\right]^T \tag{34b}$$

$$= \left[[B_1],[B_2],...,[B_i],...,\left[B_{(p+1)(q+1)}\right]\right]^T a \tag{34c}$$

Equation 34c into Eq. 33, the element stiffness matrix can be written, as

$$[K_e] = k\pi \int_0^1 \int_0^1 \sum_{i=1}^{p+1} \sum_{j=1}^{q+1} \left([B_i]^T . [D] . [B_j] \right) r . |J| d\xi . d\eta \tag{35}$$

Mass Matrix

The kinetic energy can be written

$$T(t) = \frac{1}{2} \int_{R_i}^{R_e} \int_0^H \int_O^{2\pi} \rho . \left\{ \dot{\bar{\delta}} \right\}^T . [\theta_n]^T . [\theta_n] . \left\{ \dot{\bar{\delta}} \right\} . r . dr . dz . d\theta \tag{36a}$$

$$= \frac{1}{2} \int_0^1 \int_0^1 \rho . \left\{ \dot{\bar{\delta}} \right\}^T . \left(\int_O^{2\pi} [\theta_n]^T . [\theta_n] . d\theta \right) . \left\{ \dot{\bar{\delta}} \right\} . |J| . r . d\xi . d\eta \tag{36b}$$

$$= \frac{k\pi}{2} \int_0^1 \int_0^1 \rho . \{\dot{q}\}^T . [N]^T . [N] . \{\dot{q}\} . |J| . r . d\xi . d\eta \tag{36c}$$

$$= \frac{1}{2} \{\dot{q}\}^T . \left(k\pi . \int_0^1 \int_0^1 \rho . [N]^T . [N] . |J| . r . d\xi . d\eta \right) . \{\dot{q}\} \tag{36d}$$

$$= \frac{1}{2} \{\dot{q}\}^T . [M_e] . \{\dot{q}\} \tag{36e}$$

Where:

$$[M_e] = k\pi . \int_0^1 \int_0^1 \rho . [N]^T . [N] . |J| . r . d\xi . d\eta \tag{37a}$$

$$= k\pi . \int_0^1 \int_0^1 \rho . \sum_{i=1}^{p+1} \sum_{j=1}^{q+1} [N_i]^T . [N_j] . |J| . r . d\xi . d\eta \tag{37b}$$

is the element mass matrix

Numerical Integration

The double integral appearing in the forms of the mass and stiffness matrices results in a numerical integration. For his implementation, one uses the Gauss quadrature expressed by:

$$\int_0^1 f(x) d(x) = \sum_{i=1}^{N} W_i f(x_i) \tag{38}$$

where, N is the integration points number.

After having tested several integration points numbers, the number which is a compromise between the computing time and the precision is:

$$N_{int} = p+2 \tag{39}$$

Then in order to optimize calculations, the integration points number increase automatically with the of interpolation polynomial degree.

RESULTS AND DISCUSSION

The convergence and comparison studies must be carried out to ensure the reliability of the results. The vibration frequency ω is expressed in terms of the frequency parameter

$$\Omega = \omega \cdot \sqrt{\frac{2\rho(1+\nu)}{E}} \tag{40}$$

The Poisson's ratio ν takes the value 0.3 in this study.

Convergence

The bi-hierarchical finite element is used for the first time, to study the free vibration of a very thin cylindrical shell with free boundary conditions. The external and internal radius are respectively $R_e = 1$ and $R_i = 0.99$, the shell height is $H = 2$.

Table 1 shows the convergence study of the first six modes with an increasing of the two hierarchical mode numbers p and q following respectively the radius and the axis directions for two and four elements.

The results are compared with those of the boundary collocation method (Houmat and Hutchinson, 1994) and those of ANSYS (20 harmonic and axisymmetric structural element solid with eight nodes). For the two idealization, two and four elements, an accuracy of three digits after the comma is reached for the first two modes for $p = 2$ and $q = 2$.

For modes 3, 4, 5; the convergence is reached for $p = 6$ and $q = 3$ for a 2 elements model and for $p = 4$ and $q = 2$ for a 4 elements model. The sixth mode reaches the convergence for $p = 8$ and $q = 3$ for 2 elements and $p = 6$ and $q = 2$ for 4 elements.

It is apparent that by increasing the number of elements, the hierarchical mode numbers p and q necessary to reach convergence are smaller. But the degrees of freedom number becomes more important. Indeed for mode 6 this number is of 300 for 4 elements whereas it is only of 189 for 2 elements.

The matrices size is smaller if one increases p and q rather than the elements number. Table 2 shows that the number of degrees of freedom can be easily decreased by modifying the values of p and q according to the shell geometry.

Comparison with Other Methods

In order to verify the accuracy of the bi-hierarchical finite element in solving the vibration of shells of revolution, a comparison study is conducted for different shells. A thick and a very thin cylindrical shells, a hollow cylindrical shell with varying thickness and a very thin plate. The results are compared with those of the boundary collocation method BCM, (Houmat and Hutchinson, 1994) and with those obtained by ANSYS where the harmonic and axisymmetric structural element solid with eight nodes is used.

The comparison of the frequency parameters Ω with those of the boundary collocation method (Houmat and Hutchinson, 1994) and ANSYS (32 harmonic and axisymmetric structural solid element with eight nodes) for a free thick cylindrical shell is given in Table 2. The inner radius is $R_i = 1/3$, the outer radius is $R_e = 1$ and the shell height is $H = 4/3$. Considering that the results accuracy is quickly reached for a low number of elements if one increases the number of hierarchical modes, the shell is idealized by only four bi-hierarchical finite elements with the same hierarchical modes numbers p and q according to the axial and radial directions. For this very thick cylindrical shell, $p = q = 8$.

The results given in Table 3 are in good agreement with those of the two other methods, as well for the axisymmetric case as for the non-axisymmetric case. For the high frequencies the results

Table 2: Convergence and comparison study of frequency parameter Ω for a free cylindrical shell (R_e = 1, R_i = 0.99, H = 2)

				Modes					
Element number	q	p	DOF	1	2	3	4	5	6
2	1	1	18	0.014	0.018	1.923	1.930	3.012	4.007
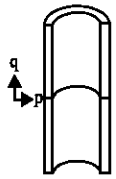	2	1	30	0.014	0.018	1057	1.347	1.882	2.614
	2	2	45	0.013	0.017	1.057	1.346	1.882	2.614
	4	2	81	0.013	0.017	0.996	1.300	1.463	1.561
	4	3	108	0.013	0.017	0.996	1.300	1.463	1.561
	6	3	156	0.013	0.017	0.996	1.300	1.461	1.531
	8	3	189	0.013	0.017	0.996	1.300	1.461	1.530
	BCM			0.013	0.017	0.996	1.300	1.465	1.529
	ANSYS			0.013	0.017	0.996	1.303	1.463	1.533
4	1	1	30	0.014	0.018	1.318	1.851	2.724	2.939
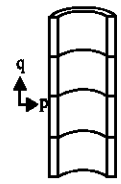	2	1	54	0.014	0.018	0.998	1.310	1.529	1.576
	2	2	81	0.013	0.017	0.998	1.309	1.526	1.571
	4	2	153	0.013	0.017	0.996	1.300	1.461	1.531
	4	3	204	0.013	0.017	0.996	1.300	1.461	1.531
	6	3	300	0.013	0.017	0.996	1.300	1.461	1.530
	8	3	396	0.013	0.017	0.996	1.300	1.461	1.530
	BCM			0.013	0.017	0.996	1.300	1.465	1.529
	ANSYS			0.013	0.017	0.996	1.303	1.463	1.533

Table 3: Comparison of frequency parameters Ù for free thick cylindrical shell (R_e =1, R_i=1/3, H = 4/3, p = 8, q = 8)

			Modes					
	Circumferential wave's number	Method	1	2	3	4	5	6
	0	Present	2.298	2.512	3.237	4.138	4.502	6.352
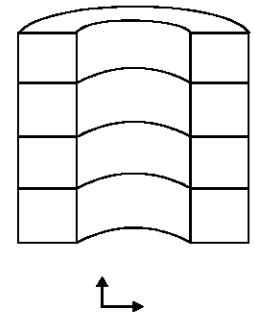		BCM	2.299	2.513	3.237	4.137	4.500	6.347
		ANSYS	2.300	2.514	3.239	4.141	4.508	6.368
	1	Present	2.124	2.716	3.305	3.448	3.892	4.645
		BCM	2.123	2.716	3.304	3.447	3.890	4.645
		ANSYS	2.125	2.718	3.307	3.452	3.895	4.650
	2	Present	1.371	1.444	3.142	3.143	4.195	4.626
		BCM	1.371	1.441	3.139	3.140	4.194	4.622
		ANSYS	1.370	1.442	3.142	3.143	4.199	4.630
	3	Present	2.820	3.079	3.762	4.285	5.531	5.716
		BCM	2.818	3.071	3.758	4.279	5.526	5.711
		ANSYS	2.818	3.074	3.761	4.286	5.538	5.727
	4	Present	4.068	4.401	4.686	5.404	6.514	6.585
		BCM	4.069	4.396	4.680	5.397	6.508	6.580
		ANSYS	4.070	4.401	4.686	5.407	6.525	6.598

approach more those of the BCM that those of ANSYS. The reason is that the warping of cross-sections is important and thus the interpolation polynomials degree must be larger to describe these modes. It is easily and automatically possible by using this bi-hierarchical finite element.

The second example is a very thin free cylindrical shell idealized by four bi-hierarchical finite elements. The outer radius is R_e = 1; the inner radius is R_i = 0.99 and the height is H = 2. The hierarchical modes number along the shell axis is q = 8 and that following the radius is p = 4. The comparison results with those of the BCM (Houmat and Hutchinson, 1994) and those of ANSYS (20 elements) are given in Table 4. The results are in perfect agreement with those of the BCM and those of ANSYS.

The third example is thick free hollow cylindrical shell with varying thickness is considered. Along the axis the inner radius is R_i = 0.6 and the outer radius is varying from R_e = 0,8 at the edges to R_e = 1 at the middle height. The height is H = 2. The shell being thick, one takes the same hierarchical modes numbers the p = q = 8. Each half cylindrical shell is idealized by one bi-hierarchical finite. Comparison Results with those of the BCM (Houmat and Hutchinson, 1994) and those of ANSYS

Table 4: Comparison of frequency parameters Ω for free thin cylindrical shell (R_e = 1, R_i = 0.99, H = 2,p = 4,q = 8)

			Modes					
	Circumferential wave number	Method	1	2	3	4	5	6
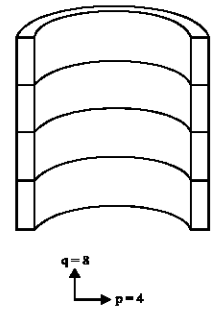	0	Present	1.576	1.613	1.618	1.620	1.625	1.636
		BCM	1.576	1.613	1.618	1.618	1.630	1.639
		ANSYS	1.577	1.613	1.618	1.621	1.625	1.637
	1	Present	1.248	1.414	1.545	1.583	1.611	1.641
		BCM	1.248	1.414	1.544	1.587	1.612	1.658
		ANSYS	1.250	1.416	1.546	1.584	1.613	1.643
	2	Present	0.013	0.017	0.995	1.300	1.461	1.530
		BCM	0.013	0.022	0.996	1.297	1.465	1.529
		ANSYS	0.013	0.017	1.000	1.303	1.463	1.533
	3	Present	0.037	0.044	0.660	1.059	1.292	1.422
		BCM	0.037	0.048	0.662	1.056	1.297	1.419
		ANSYS	0.037	0.044	0.665	1.063	1.295	1.425
	4	Present	0.071	0.079	0.453	0.838	1.114	1.294
		BCM	0.072	0.083	0.458	0.835	1.121	1.291
		ANSYS	0.071	0.079	0.457	0.843	1.118	1.298

Table 5: Comparison of frequency parameters Ω for a free thick hollow cylindrical shell of varying thickness (R_e varying, R_i = 0.6, H = 2, p = 8, q = 8)

			Modes					
	Circumferential wave's number	Method	1	2	3	4	5	6
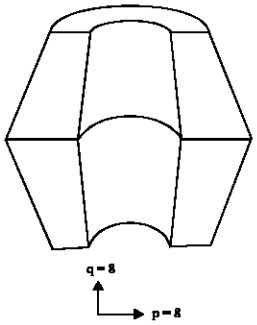	0	Present	2.006	2.193	2.366	2.844	3.273	3.880
		BCM	2.007	2.195	2.367	2.839	3.279	3.896
		ANSYS	2.007	2.193	2.367	2.846	3.275	3.889
	1	Present	1.629	1.996	2.518	2.832	3.370	3.382
		BCM	1.627	2.002	2.518	2.835	3.370	3.384
		ANSYS	1.629	1.997	2.519	2.839	3.373	3.386
	2	Present	0.644	0.761	1.853	2.466	2.967	3.309
		BCM	0.646	0.760	1.861	2.464	2.963	3.308
		ANSYS	0.644	0.761	1.855	2.468	2.976	3.312
	3	Present	1.641	1.762	2.444	3.356	3.767	4.228
		BCM	1.641	1.755	2.449	3.348	3.761	4.228
		ANSYS	1.642	1.763	2.448	3.365	3.774	4.239
	4	Present	2.811	2.904	3.451	4.229	4.996	5.163
		BCM	2.811	2.890	3.453	4.214	4.991	5.166
		ANSYS	2.815	2.908	3.458	2.242	5.009	5.188

(16 elements) are given in Table 5. The same observation is made as for the two other examples. The results agree very well with those of the BCM and those of ANSYS, which shows the power of this element.

Finally, to verify the accuracy of the bi-hierarchical finite element in solving the vibration of flattened shells of revolution, a very thin free circular plate is considered. The plate is idealized by two bi-hierarchical finite elements The radius is R =1 and the thickness is H = 0.05. The hierarchical modes numbers along the shell thickness is q = 3 and that following the radius is p = 12. The comparison results with those of the BCM (Houmat and Hutchinson, 1994) and those of ANSYS (20 elements) are given in Table 6. The results are in perfect agreement with those of the BCM and those of ANSYS.

Applications

The frequency parameter variation against the circumferential waves number is carried out by using this element for two examples. A very thin free cylindrical shell (height = 2, thickness = 0.01) and the same cylinder but clamped at its base.

The vibration characteristics of a cylindrical shell could be evaluated by observing the radial deformation. Figure 4 shows the circumferential node patterns of a cylindrical shell, n being the circumferential waves number.

Table 6: Comparison of frequency parameters Ω for a free thin circular plate (Thickness = 0.05, Radius = 2, p = 12, q = 3)

	Circumferential		Modes					
	wave's number	Method	1	2	3	4	5	6
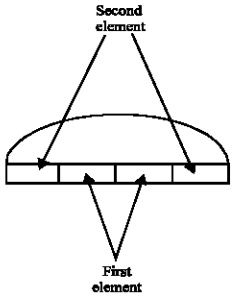	0	Present	0,219	0.924	2.070	3.463	3.611	9.104
		BCM	0,219	0.923	2.066	3.463	3.595	9.104
		ANSYS	0,219	0.924	2.070	3.463	3.610	9.108
	1	Present	0.495	1.424	2.734	2.772	4.493	5.964
		BCM	0.494	1.419	2.734	2.761	4.464	5.964
		ANSYS	0.495	1.425	2.734	2.774	4.493	5.965
	2	Present	0.130	0.846	1.990	2.345	3.532	4.244
		BCM	0.136	0.840	1.977	2.345	3.506	4.244
		ANSYS	0.130	0.846	1.990	2.345	3.533	4.245
	3	Present	0.301	1.262	2.613	3.601	4.340	5.834
		BCM	0.308	1.251	2.590	3.601	4.296	5.834
		ANSYS	0.300	1.261	2.612	3.601	4.335	5.835
	4	Present	0.525	1.736	3.287	4.689	5.194	7.437
		BCM	0.532	1.718	3.253	4.689	5.126	7.438
		ANSYS	0.525	1.734	3.285	4.689	5.180	7.439

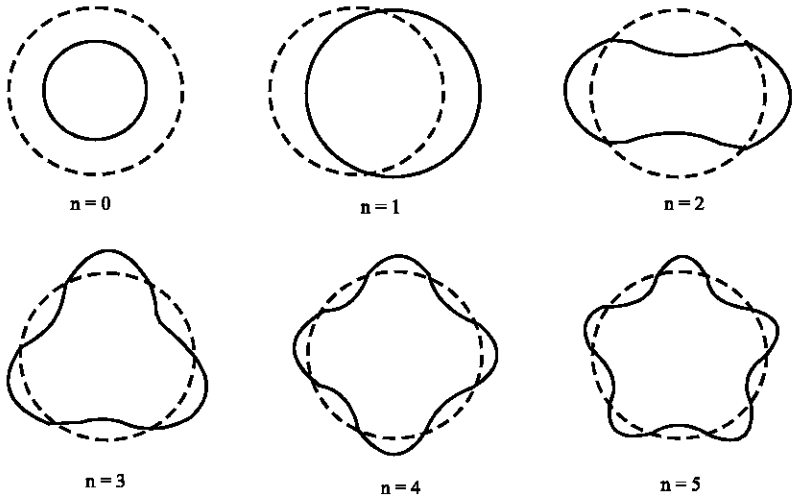

Fig. 4: Circumferential node patterns of a cylindrical shell

For n = 0, the circumferential nodal pattern is a circle, indicating that this mode is an extensional mode referred to as breathing type mode. n = 1 indicates two crossings between the deformed and original shapes, n = 2 indicates four crossings.

The lowest frequency does not occur at the lowest values of n. For example, for the thin free-clamped cylindrical shell, the lowest frequency occurs when n = 4, this phenomenon can be explained by considering the strain energy of the middle surface under both bending and stretching (Kraus, 1967).

Figure 5 shows for the free cylindrical shell, that the modes have almost the same frequency parameter for the axisymmetric case (circumferential waves number equal to zero). Starting from a number of circumferential waves equal to 1 (non-axisymmetric case) the frequency parameters decrease gradually except for the first two modes frequency parameters decrease quickly to the value 2 then increase gradually.

The cylindrical shell with clamped edge (Fig. 6), is a similar case except for the modes 1 and 2 whose frequency parameters increase between values 0 and 1 of the circumferential waves number then decrease gradually.

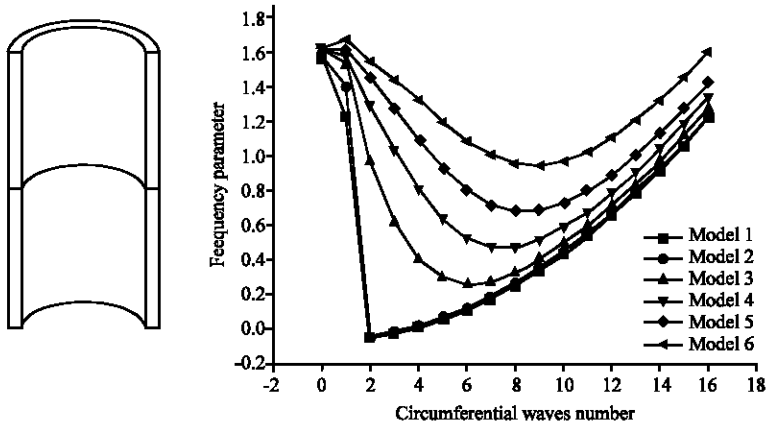

Fig. 5: Frequency parameters variation against the circumferential waves number of a very thin free-fre cylindrical shell (thickness = 0.01, height = 2, p = 2, q = 12)

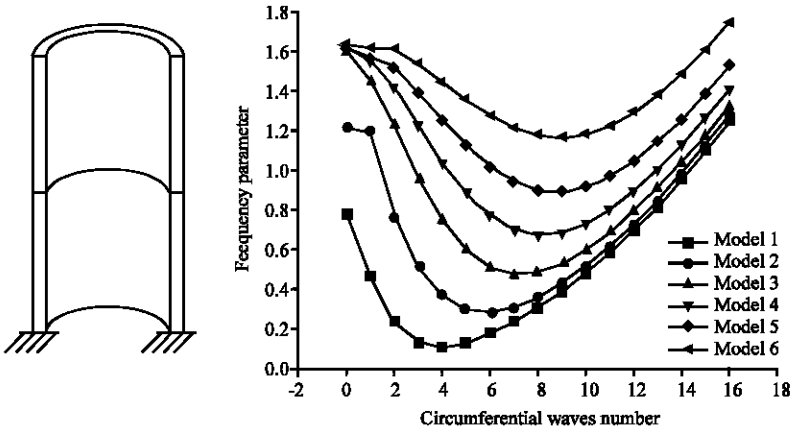

Fig. 6: Frequency parameters variation against the circumferential waves number base of a free-clamped very thin cylindrical shell (thickness = 0.01, height = 2, p = 2, q = 12)

CONCLUSION

The bi-hierarchical finite element presented in this study is able to give accurate frequencies for shells of revolution of an unspecified shape. The results show clearly that this element can be easily used for the extreme cases of very thin or very thick shells of revolution. With this element one is not constrained any more to have the same number of hierarchical modes in the two main directions of the radial and axial shells of revolution. Indeed, if the shapes and dimensions change (thick or thin shells) the hierarchical modes number can change very easily. This element can also be used to idealize a composed shell, plate linked to cylindrical shell for example. Finally this bi-hierarchical finite element allows triple increase in the accuracy, finite elements number and radial and axial hierarchical modes numbers.

REFERENCES

Babuska, I. and B. Szabo, 1982. On the rates of convergence of the finite element method. Int. J. Num. Meth. Eng., 18: 323-341.

Batoz, J.L. and G. Dhatt, 1992. Modélisation des structures par éléments finis. Hermes Edition. Coques (In French), Paris, pp: 1-3.

Houmat A. and J.R. Hutchinson, 1994. Free vibration of bodies of revolution by boundary collocation. J. Sound Vibrations, 171: 35-48.

Houmat, A., 2004. Three dimensional hierarchical finite element free vibration analysis of annular sector plates. J. Sound Vibrations, 276: 181-193.

Kang, J.H. and A.W. Leissa, 2005a. Free vibration analysis of complete paraboloidal shells of revolution with variable thickness and solid paraboloids from a three-dimensional theory. Comput. Struct., 183: 2594-2608.

Kang, J.H. and A.W. Leissa, 2005b. Free vibration of thick complete conical shells of revolution from a three-dimensional theory. J. Applied Mech., 72: 797-800.

Kang, J. H. and A.W. Leissa, 2005c. Three-dimensional vibration of thick hyperboloidal shells of revolution. J. Sound Vibrations, 282: 277-296.

Kraus, H., 1967. Thin Elastic Shells. 1st Edn. John Wiley, New York .

Leissa, W., 1999. Three-dimensional vibration analysis of thick shells of revolution. J. Eng. Mech., 125: 1365-1371.

Özakça, M. and E. Hinton, 1993. Free vibration analysis and optimisation of axisymmetric plates and shells-I. Finite element formulation. Comput. Struct., 52: 1181-1197.

Shim, H.J. and J.H. Kang, 2004. Free vibration of solid and hollow hemi-ellipsoids of revolution from a three-dimensional theory. Int. J. Eng. Sci., 42: 1793-1815.

Szabo, B.A., 1990. The use of a priori estimates in engineering computations. Comp. Meth. Applied Mech. Eng., 82: 139-154.

Szabo, B.A. and I. Babuska, 1991. Finite Element Analysis. 1st Edn. John Wiley and Sons, New York, USA .

Tan, D.Y., 1998. Free vibration analysis of shells of revolution. J. Sound Vibrations, 213: 15-33.

Young, P.G., 2000. Application of a three-dimensional shell theory to the free vibration of shells arbitrarily deep in one direction. J. Sound Vibrations, 238: 257-269.